

PAPER • OPEN ACCESS

## Semi-grand canonical Monte Carlo simulation for derivation of thermodynamic properties of binary alloy

To cite this article: Kensho Ueno and Yasushi Shibuta 2019 *IOP Conf. Ser.: Mater. Sci. Eng.* **529** 012037

View the [article online](#) for updates and enhancements.



**IOP | ebooks™**

Bringing you innovative digital publishing with leading voices to create your essential collection of books in STEM research.

Start exploring the collection - download the first chapter of every title for free.

# Semi-grand canonical Monte Carlo simulation for derivation of thermodynamic properties of binary alloy

**Kensho Ueno and Yasushi Shibuta**

Department of Materials Engineering, The University of Tokyo, 7-3-1, Hongo, Bunkyo-ku, Tokyo 113-8656, Japan

E-mail; ueno@mse.mm.t.u-tokyo.ac.jp

**Abstract.** Semi-grand canonical Monte Carlo (SGCMC) simulations are performed to derive thermodynamic properties of binary alloy from atomistic-based simulations. Particularly, solidus and liquidus compositions are directly derived for Fe-Cr alloy described by two different EAM potentials. Although the SGCMC simulation can derive relationship between the free energy and composition at any temperature straightforwardly, partial phase diagram obtained from SGCMC simulations strongly depends on the choice of interatomic potential.

## 1. Introduction

Solid-liquid interfacial properties have a great influence on the solidification microstructure [1-3]. Therefore, it is important to know interfacial properties such as the interfacial energy and mobility. However, it is not easy to experimentally obtain such interfacial properties with high accuracy. Therefore, in recent years, derivation of these properties by numerical analysis method such as molecular dynamics method (MD) is becoming popular. At present, there are many reports on interfacial properties of pure metals based on MD simulations [2,3]. However, there are not so many reports on those of alloy systems since derivation techniques on the estimation of interfacial properties of the alloy system are not established yet. For example, it is difficult to handle the solute distribution at the solid-liquid interface in the MD simulation since time scale of diffusion is much longer than that of a conventional MD simulation. Moreover, it is not straightforward to deterministically define the entropy of a system from the coordinate and velocity of atoms obtained by MD simulations since the number of states cannot



be defined in principle for a system governed by the classical equation of motion [4]. This makes it difficult to validate the accuracy of the interatomic potential of alloy systems. Therefore, a Monte Carlo (MC) simulation is often employed as an alternative technique to derive properties of alloys although it is not straightforward for MC simulations to treat dynamics of the interface. For example, a Metropolis Monte Carlo (MMC) simulation in conjunction with an atoms swap technique is often used to estimate equilibrium concentrations of a solid-liquid biphasic system of a binary alloy at a finite temperature [5].

Moreover, the Gibbs free energy of mixing can be derived from a semi-grand canonical MC (SGCMC) simulation [6-8], in which an equilibrium concentration for given chemical potential difference is obtained. In this paper, we performed SGCMC simulations to derive solidus-liquidus composition of binary alloy, which is an important thermodynamic factor determining solid-liquid interfacial properties. Here, Fe-Cr alloy described by for several interatomic potentials is employed as a model system since the partition coefficient changes significantly between Fe-rich and Cr-rich compositions.

## 2. Methodology

In this study, SGCMC and MD simulations are performed using LAMMPS (Large-scale Atomic/Molecular Massive Parallel Simulator) [9]. The EAM (embedded atom method) potentials fitted by Bonny et al. [10] (abbreviated as EAM(BPTM)) and by Stukowski et al. [11] (abbreviated as EAM(SSEC)) are employed as the interatomic potential of Fe-Cr alloy. Parameter files for the EAM potentials from the database of NIST-IPR project [12] are utilized for simulations by the LAMMPS. The Nose-Hoover thermostat and barostat [13,14] are employed to control temperature and pressure in MD simulations. We follow literatures [6-8] for practical procedure of SGCMC simulations.

## 3. Results and discussion

### 3.1 Melting point, enthalpy, and difference in Gibbs free energy between solid and liquid

Prior to SGCMC simulations of derivation of solidus and liquidus compositions for Fe-Cr alloy, melting points of pure Fe and difference in Gibbs free energy between solid and liquid for EAM potentials employed in this work are estimated by MD simulations. For the estimation of melting point, the convergence temperature technique [15,16] is performed as follows. Two bcc crystals consisting of  $75 \times 25 \times 25$  unit cells (93750 atoms) for the EAM(BPTM) potential and  $100 \times 25 \times 25$  unit cells (250000 atoms) for the EAM(SSEC) potential are annealed at 500 and 3000 K for 10 ps with the number of atoms, volume and temperature (NVT)-constant ensemble to obtain solid and liquid structures, respectively. Then, these structures are connected with the (100) plane appearing on the interface and the energy minimization is performed to avoid the unexpected proximity of atoms at the solid-liquid interface. The obtained these structures are used as the initial configuration of the following simulations.

The solid-liquid biphasic system of pure Fe is relaxed with the number of atoms, pressure and temperature (NPT)-constant ensemble for 25 ps at 1700, 1750 and 1800 K. Then, the systems are relaxed with the number of atoms, pressure and enthalpy (NPH)-constant ensemble for subsequent 1975 ps. The pressure is maintained at 0 Pa in all processes. In this technique, the convergence temperature is regarded as the melting point of the target material [15,16]. Figure 1 shows temperature as a function of time for the solid-liquid biphasic systems of pure Fe described by EAM (BPTM) and EAM(SSEC) potentials, respectively. Melting points are estimated to  $1770 \pm 10$  K for EAM(BPTM) and  $1770 \pm 10$  K for EAM(SSEC), respectively, which are closed to the experimental value (1811 K).

Next, the difference in Gibbs free energy between solid and liquid  $\Delta G_{SL} (= G_L - G_S)$  for pure Fe is estimated using the following Gibbs-Helmholtz relation:

$$\left[ \frac{\partial}{\partial T} \left( \frac{\Delta G_{SL}}{T} \right) \right]_P = - \frac{\Delta H_{SL}}{T^2}. \quad (1)$$

where  $\Delta H_{SL} (= H_L - H_S)$  is the difference in enthalpy between solid and liquid and  $T$  is the temperature. Since  $\Delta G_{SL}$  becomes zero at the melting point  $T_M$ , the following relation is obtained:

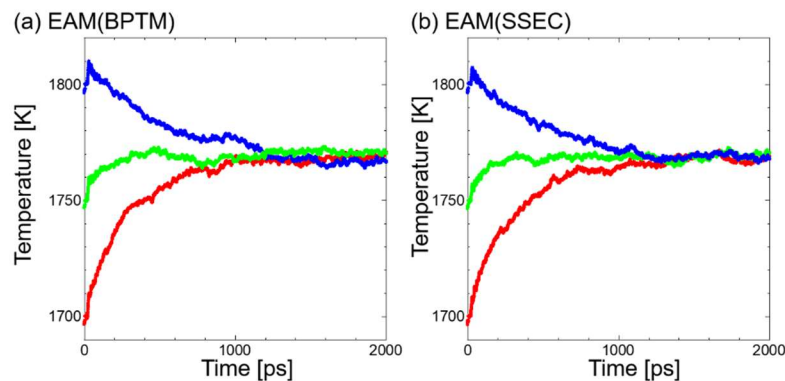


**Figure 1.** Time change of temperature for solid-liquid biphasic system of pure Fe described by (a) EAM(BPTM) and (b) EAM(SSEC) potentials.

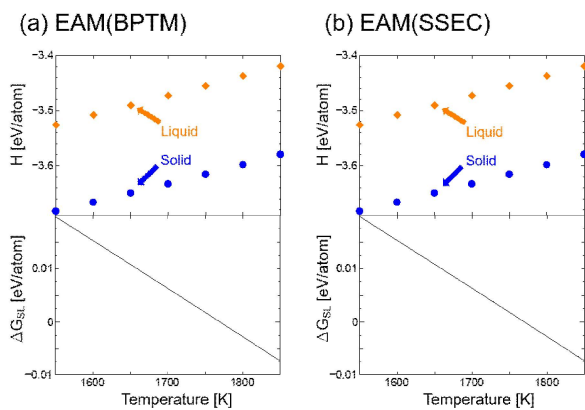


**Figure 2.** (Top) Enthalpy of solid and liquid systems and (bottom) difference in Gibbs free energy between solid and liquid for pure Fe described by (a) EAM (BPTM) and (b) EAM (SSEC) potentials.

$$\Delta G_{\text{SL}}(T) = T \int_T^{T_M} \frac{\Delta H_{\text{SL}}(T')}{T'^2} dT'. \quad (2)$$

Since the enthalpy is directly calculated from MD simulation,  $\Delta G_{\text{SL}}$  can be estimated from the difference in enthalpy between solid and liquid, which is calculated as follows. For a solid system, a bcc crystal consisting of  $20 \times 20 \times 20$  unit cells (16000 atoms) is annealed at various temperatures between 1550 and 1850 K at intervals of 50 K with the NPT-constant ensemble to calculate enthalpy. A liquid structure obtained by pre-anneal of the bcc crystal at 5000K for 10 ps is annealed at same temperatures in the solid system. The enthalpy of solid and liquid system obtained by MD simulations and the difference in Gibbs free energy between solid and liquid for pure Fe derived from Equation (2) are shown in Figure 2.

### 3.2 Solidus and liquidus compositions from SGCMC simulations

Then, SGCMC simulations are performed using a bcc crystal consisting of  $20 \times 20 \times 20$  unit cells (16000 atoms). A liquid structure obtained by pre-anneal of the bcc crystal at 5000K for 10 ps is used for calculations of liquid system. In a SGCMC simulation, an equilibrium concentration is obtained for the given chemical potential difference  $\Delta\mu$  at given temperature. Here, SGCMC simulations between  $\Delta\mu = -1.0$  and  $1.0$  eV/atom at intervals of  $0.1$  eV/atom are performed at various temperatures. Figure 3(a) and 3(b) show the relationship between  $\Delta\mu$  and equilibrium Cr composition  $X_{\text{Cr}}$  at 1800 and 1900 K for EAM(BPTM) potential and 1900 and 2000 K for EAM(SSEC) potential, respectively. Plots obtained from SGCMC simulations are fitted to the following equation to obtain the fitting parameters  $A_i$  ( $i = 0, 1, \dots, n$ ).

$$\Delta\mu = kT \ln \left( \frac{x_{\text{Cr}}}{1-x_{\text{Cr}}} \right) + \sum_{i=0}^n A_i x_{\text{Cr}}^i, \quad (3)$$

where  $k$  is the Boltzmann constant. Here,  $n = 5$  is employed. Once fitting parameters are obtained, a Gibbs free energy of mixing is described as

$$\Delta G_{\text{mix}} = kT [x_{\text{Cr}} \ln x_{\text{Cr}} + (1-x_{\text{Cr}}) \ln(1-x_{\text{Cr}})] + \sum_{i=0}^n \frac{A_i x_{\text{Cr}}^{i+1}}{(i+1)}. \quad (4)$$

Figure 3(c) and 3(d) shows the Gibbs free energy of mixing for solid and liquid phases of the Fe-Cr alloy for corresponding temperatures. Here, Gibbs free energy of mixing for solid at  $X_{\text{Cr}} = 0$  is defined as a reference value (i.e. zero). Therefore, Gibbs free energy of mixing for liquid at  $X_{\text{Cr}} = 0$  takes a value of  $\Delta G_{\text{SL}}$ , which is derived from Equation (2). Finally, solidus and liquidus compositions are derived from the contact points of the common tangent line as shown in the figure.

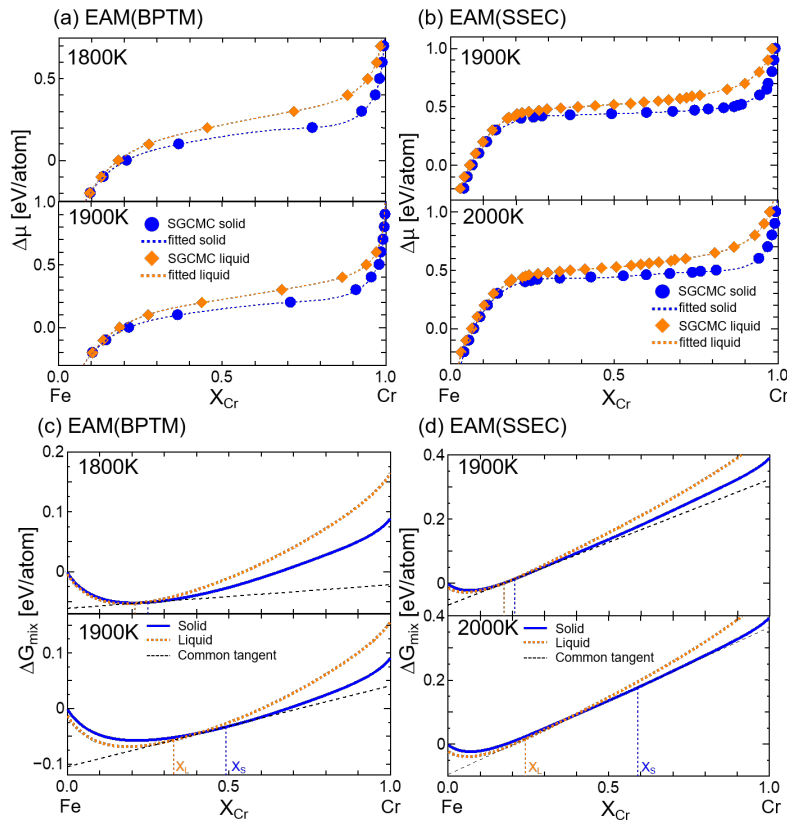


**Figure 3.** (a)(b) Relationship between  $\Delta\mu$  and equilibrium Cr composition and (c)(d) Gibbs free energy of mixing for solid and liquid phases of the Fe-Cr alloy at 1800 and 1900 K for EAM(BPTM) potential and 1900 and 2000 K for EAM(SSEC) potential.

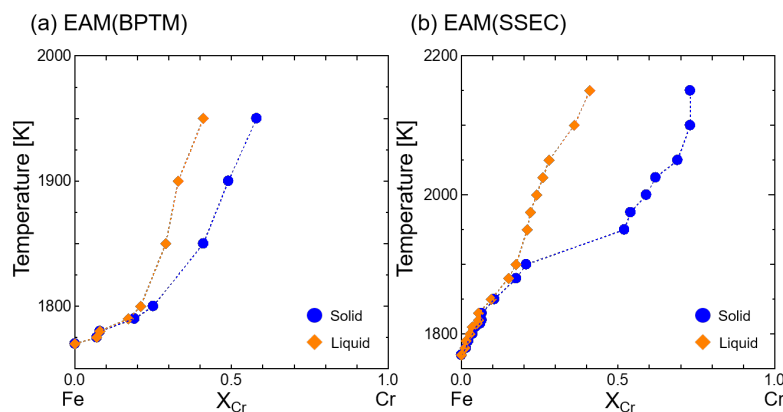


**Figure 4.** Partial phase diagram from SGCMC simulations: (a) EAM(BPTM) potential and (b) EAM(SSEC) potential.

Solidus and liquids composition at various temperatures can be obtained by repeating SGCMC simulation with different temperatures. Figure 4 shows the partial phase diagram obtained by SGCMC simulations. In general, there is no significant difference between solidus and liquidus composition at

the Fe-rich compositions, whereas there is large difference in it at the Cr-rich compositions for both interatomic potentials. However, there is a large difference in shape of solidus and liquidus lines between EAM(BPTM) and EMA(SSEC) potentials. Especially, solidus and liquidus compositions at high temperature are not well defined for the EAM(BPTM) potential. It is not straightforward to develop the interatomic potential which reproduce solidus and liquidus compositions at high temperature since these properties are not explicit in the interatomic potential curve itself.

#### 4. Conclusions

In this study, SGCMC simulations are performed to derive solidus and liquidus composition of binary alloys described by two different EAM potentials for Fe-Cr alloy. Although the SGCMC simulation derives relationship between the free energy and composition at any temperature straightforwardly, obtained results strongly depend on the choice of interatomic potential. Moreover, this technique is not used straightforwardly when the relationship between  $\Delta\mu$  and equilibrium is not monotonic, which causes a miscibility gap in the phase diagram. Therefore, it is essential to establish methodology for derivation of phase diagram from interatomic potential to discuss its reliability. Further investigation is needed to fill the gap between atomistic-based simulations and macroscopic thermodynamics for alloy systems.

#### References

- [1] Dantzig J A and Rappaz M, *Solidification* 2009 (Lausanne: EPFL Press) pp. 287-344.
- [2] Shibuta Y, Ohno M and T. Takaki 2015 *JOM* **67** 1793.
- [3] Shibuta Y, Ohno M and T. Takaki 2018 *Adv. Theo. Sim.* **1** 1800065.
- [4] Shibuta Y 2019 *Mater. Trans.* submitted.
- [5] Ueno K and Shibuta Y 2018 *Materialia* **4** 553.
- [6] Ramalingam H, Asta M, van de Walle A and Hoyt J J 2002 *Interface Sci.* **10** 149.
- [7] Becker C A, Asta M, Hoyt J J and Foiles S M 2006 *J. Chem. Phys.* **124** 164708.
- [8] Becker C A, Olmsted D L, Asta M, Hoyt J J and Foiles S M 2009 *Phys. Rev. B* **79** 054109.
- [9] Plimpton S J 1995 *J. Comput. Phys.* **117** 1, <http://lammps.sandia.gov>.
- [10] Bonny G, Pasianot RC, Terentyev D and Malerba L 2011 *Philos. Mag.* **91** 1724.
- [11] Stukowski A, Sadigh B, Erhart P and Caro A 2009 *Modeling Simul. Mater. Sci. Eng.* **17** 075005.
- [12] Becker C A, Tavazza F, Trautt Z T and Buarque de Macedo R A 2013 *Curr. Opin. Solid State Mater. Sci.* **17** 277, <http://www.ctcms.nist.gov/potentials>.
- [13] Nose S 1984 *J. Chem. Phys.* **81** 511.
- [14] Hoover W G 1985 *Phys. Rev. A* **31** 1695.
- [15] Shibuta Y and Suzuki T 2007 *Chem. Phys. Lett.* **445** 265.
- [16] Shibuta Y, Takamoto S and Suzuki T 2008 *ISIJ Int.* **48** 1582.